Science of the Total Environment 927 (2024) 172151

Contents lists available at ScienceDirect

Science of the Total Environment

journal homepage: www.elsevier.com/locate/scitotenv

Radioactivity from oil and gas produced water accumulated in freshwater mussels

Katharina Pankratz, Nathaniel R. Warner *

Civil & Environmental Engineering, The Pennsylvania State University, 212 Sackett Building, University Park, PA 16802-1408, United States of America

HIGHLIGHTS

- Discharge of oil and gas produced water (OGPW) led to increased radium in mussels.
- Shell & tissue metal/Ca, $^{87}Sr/^{86}Sr$, and $^{228}Ra/^{226}Ra$ indicate areas impacted by OGPW.
- Elemental & isotopic signatures persist in mussels years after discharges ceased.

GRAPHICAL ABSTRACT

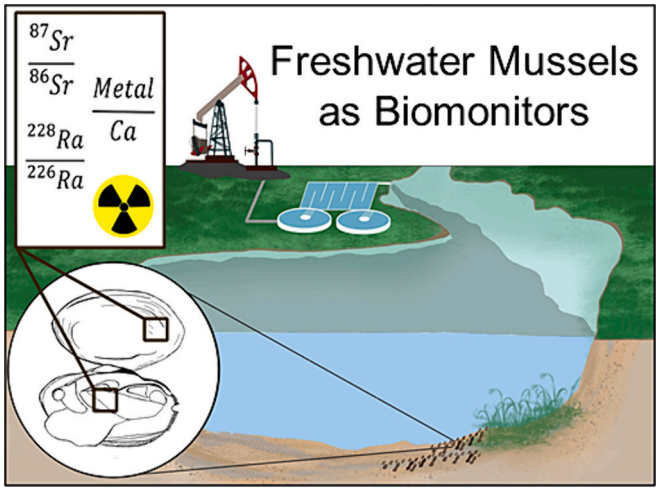

ARTICLE INFO

Editor: Daniela Maria Pampanin

Keywords:
Brine
Biomonitor
Biological indicator
Bivalve
Radium
NORM

ABSTRACT

Legacy disposal of oil and gas produced water (OGPW) to surface water has led to radium contamination in streambed sediment creating a long-term radium source. Increased radium activities pose a potential health hazard to benthic organisms, such as freshwater mussels, as radium is capable of bioaccumulation. This project quantifies the impact of OGPW disposal on adult freshwater mussels, *Eurynia dilatata*, which were examined along the Allegheny River adjacent to a centralized waste treatment facility (CWT) that historically treated and then discharged OGPW. Radium isotopes (^{226}Ra and ^{228}Ra) were measured in streambed sediment, mussel soft tissue, and mussel hard shell collected upstream, at the outfall, 0.5 km downstream, and 5 km downstream of the CWT. Total radium activity was significantly higher ($p < 0.05$) in mussel tissue (mean = 3.44 ± 0.95 pCi/g), sediment (mean = 1.45 ± 0.19 pCi/g), and hard shell (mean = 0.34 ± 0.11 pCi/g) samples 0.5 km downstream than background samples collected upstream (mean = 1.27 ± 0.24; 0.91 ± 0.09; 0.10 ± 0.02 pCi/g respectively). Mussel shells displayed increased ^{226}Ra activities up to 5 km downstream of the original discharge. Downstream soft tissue and hard shell $^{87}Sr/^{86}Sr$ ratios, as well as hard shell metal/calcium (e.g., Na/Ca; K/Ca;

* Corresponding author.
E-mail address: nrw6@psu.edu (N.R. Warner).

https://doi.org/10.1016/j.scitotenv.2024.172151
Received 18 January 2024; Received in revised form 21 March 2024; Accepted 30 March 2024
Available online 2 April 2024

Mg/Ca) and $^{228}Ra/^{226}Ra$ ratios demonstrated trends towards values characteristic of Marcellus OGPW. Combined, this study demonstrates multiple lines of evidence for radium retention and bioaccumulation in freshwater mussels resulting from exposure to Marcellus OGPW.

1. Introduction

In the Northern Appalachian Basin, water injected for oil and gas drilling and extraction activities encounters high salinity pore fluids containing high total dissolved solids (TDS) and radium concentrations (Dresel et al., 2010; Rowan et al., 2011). These highly saline and radioactive fluids come to the surface along with the targeted resource and are known as oil and gas produced water (OGPW). The elevated TDS predominantly consists of sodium (Na^+), calcium (Ca^{2+}), and chloride (Cl^-) ions with other inorganic constituents potassium (K^+), magnesium (Mg^{2+}), strontium (Sr^{2+}), barium (Ba^{2+}), iron (Fe^{2+}), manganese (Mn^{2+}), and bromide (Br^-) still greatly surpassing U.S. drinking water standards (Haluszczak et al., 2013). Of particular concern is elevated concentrations of radioactivity in the form of radium. Two long lived isotopes of radium, ^{226}Ra ($t_{1/2} = 1602$ yrs.) and ^{228}Ra ($t_{1/2} = 5.7$ yrs.), are sourced via radioactive decay from uranium-238 (^{238}U) and thorium-232 (^{232}Th), respectively. The less abundant short-lived isotopes of radium, ^{223}Ra ($t_{1/2} = 11.4$ days) and ^{224}Ra ($t_{1/2} = 3.63$ days), sourced from ^{235}U and ^{232}Th respectively are not included in this analysis due to their short half-lives and quick degradation providing uncertainty in environmental samples taken outside of this time frame, as well as general lack of measurements in OGPW literature (Barker and Thatcher, 1957; Nelson et al., 2015). Unlike its parent elements, radium is soluble under reducing conditions found at depth, and can be incorporated into high salinity pore fluids, which are then mobilized to the surface as OGPW (Gonneea et al., 2008; Landis et al., 2018a; Landis et al., 2018b). Total radium activities ($^{226}Ra + ^{228}Ra$) from OGPW vary with source reservoir but have been reported well above 10,000 pCi/L (Barbot et al., 2015; Rowan et al., 2011) while standardized drinking water limits regulate to 5 pCi/L. Radioactivity associated with OGPW is referred to as naturally occurring radioactive materials (NORM).

One oil and gas target with notably high NORM is the Marcellus Formation in the Appalachian region. Marcellus OGPW has reported maximum combined radium ($^{226}Ra + ^{228}Ra$) activities up to 19,600 pCi/L (Shih et al., 2015). This formation is predominantly a shale source rock with high ^{238}U deposits compared to ^{232}Th resulting in increased ^{226}Ra activities compared to ^{228}Ra. Therefore, a low isotopic ratio ($^{228}Ra/^{226}Ra < 0.3$) is observed in Marcellus Shale OGPWs compared to median OGPW ratios ($^{228}Ra/^{226}Ra = 1$) typical of many sandstone reservoirs in the Appalachian Basin (Asikainen, 1981; Dresel et al., 2010; Rowan et al., 2011). In addition to possessing a distinctive radium isotopic ratio, the Marcellus produced waters exhibit unique strontium isotopic ratios ($^{87}Sr/^{86}Sr < 0.712117$), significantly divergent from values recorded in Pennsylvania abandoned mine drainages or upper Devonian brines originating from sandstone reservoirs (Chapman et al., 2012, 2013). These characteristics lend not only $^{228}Ra/^{226}Ra$, but also $^{87}Sr/^{86}Sr$ to behave as a sensitive indicator for Marcellus OGPW contamination (Kolesar Kohl et al., 2014; McDevitt et al., 2020).

Once at the surface, the disposal of OGPW is regulated. In some regions, OGPW is disposed to surface water after treatment at centralized waste treatment facilities (CWTs) under National Pollutant Discharge Elimination System (NPDES) permits detailed in the Clean Water Act sections 301 and 402 (U.S. Environmental Protection Agency, 2020; U.S Environmental Protection Agency and Engineering and Analysis Division, 2018). OGPW disposal to surface water in Pennsylvania is decreasing and currently prohibits unconventional OGPW such as from the Marcellus Shale, but from 2008 to 2011 Pennsylvania streams saw disposal of a significant volume of Marcellus OGPW (Van Sice et al., 2018; Wilson and Vanbriesen, 2012). While disposal to surface water is no longer permitted, the historical discharge proved detrimental to water and sediment quality as the legacy radium and strontium contamination is still measurable (Lauer et al., 2018; Van Sice et al., 2018).

OGPW discharged to streams pose a risk to water resources even after treatment (Ferrar et al., 2013). Discharges often increased Cl^-, Sr^{2+}, and Ba^{2+} surface water concentrations significantly above drinking water and human health standards (Ferrar et al., 2013; Haluszczak et al., 2013). OGPW treatment in CWT facilities often reduces radium activity by >90 % before discharge to surface streams; however, even lower concentrations of radium in the discharge lead to elevated radium (up to 200 times background levels) in areas directly downstream of a CWT discharge (Warner et al., 2013). Elevated radium activities have been seen as far as 31 km downstream of the initial discharge at 1.5 times above background levels (Van Sice et al., 2018) and as deep as 30 cm near the discharge point (McDevitt et al., 2019), indicating surface disposal of OGPW changes radium activity in sediment at the watershed scale. Much of the impact to sediments in Pennsylvania can be linked to disposal of Marcellus wastewater from 2008 to 2011 through isotopic tracers such as $^{228}Ra/^{226}Ra$ that reflect Marcellus OGPW signatures (Lauer et al., 2018), utilizing sediment cores to correlate periods of time when Marcellus OGPW was disposed at greatest volumes (Burgos et al., 2017).

The species and form of radium changes from OGPW extraction to deposition in the aquatic surface sediment. Radium that is brought to the surface in highly saline OGPW is predominantly in its dissolved ionic Ra^{2+} form. Once OGPW is treated and disposed to surface water, radium becomes highly diluted and may form complexes with Cl^-, SO_4^{2-}, and CO_3^{2-} ions near the outfall (Rosenberg et al., 2011a; Rowan et al., 2011). The presence of high sulfate content in most western Pennsylvania surface waters leads to rapid radium co-precipitation as radiobarite (Ba, Sr,Ra)SO_4 (McDevitt et al., 2019; Rosenberg et al., 2011b; Van Sice et al., 2018). As radium travels downstream, it sorbs to fine grained sediment containing Fe and Mn oxyhydroxides. Remobilization of the radium from radiobarite or Fe and Mn oxyhydroxides is possible with small changes to pH or oxidation-reduction potential over time (Van Sice et al., 2018). These characteristics lead radium to be a long-term pollution source in sediment downstream of OGPW impacted areas. Continuous radium exposure could pose a threat to aquatic and human health as radium becomes bioavailable and accumulates in aquatic species, such as freshwater bivalves.

Freshwater mussels are filter-feeding bivalve aquatic organisms that burrow into streambed sediment and remain sessile with lifespans of decades to centuries (Strayer, 2014; Yeager et al., 1994). Due to their sessile and filter-feeding nature, freshwater mussels cannot escape local pollution sources and impaired water quality. The outer hard shell is the animals' main defense and is primarily composed of precipitated biogenic calcium carbonate ($CaCO_3$) in the form of calcite and aragonite. This shell is continuously secreted outward over time as the bivalve grows (Dailianis, 2011). Elements with a similar divalent structure to Ca^{2+} (e.g., Ba^{2+}, Sr^{2+}, Ra^{2+}) (Geeza et al., 2018a) and even rare earth elements (Merschel and Bau, 2015) may be incorporated at low concentrations into the shell structure during formation dependent on calcification rates and bioavailable elements in the surrounding environment (Takesue et al., 2008). Less is understood regarding contaminant partitioning into the soft tissue of the animal; however, studies have reported the retention of nitrogen and carbon isotopes (Gustafson et al., 2007), heavy metals (Wagner and Boman, 2004), organic industrial pollutants and pesticides (Metcalfe and Charlton, 1990), and other emerging contaminants of concern (Ismail et al., 2014). Radium can also be incorporated in the flesh and acts as a chemical analogue for calcium

with assumed accumulation and retention occurring in calcium phosphate granules (Bollhöfer et al., 2011; Jeffree and Simpson, 1984). Accounting for these characteristics, freshwater mussels exposed to OGPW disposals may be susceptible to bioaccumulation of contaminants leading to consequent health risks and further population decline.

Previous studies demonstrated that $^{87}Sr/^{86}Sr$ and Sr/Ca ratios measured in the hard shell and soft tissue of mussels exposed to Marcellus OGPW can reliably trace the quantity (McDevitt et al., 2021) and duration (Geeza et al., 2018a,b) of produced water exposure. Freshwater mussels exposed to OGPW from the Utica/Point Pleasant formation accumulated Sr^{2+}, Ba^{2+}, and cyclic hydrocarbons in their soft tissue at concentrations reflective of the degree of exposure (Piotrowski et al., 2020) in a laboratory setting, and juvenile mussels, which are less resistant to contaminants compared to adults, have experienced increased mortality downstream of OGPW discharges (Patnode et al., 2015). Given the impacts OGPW disposal has on freshwater mussels and the elevated sediment radium activities downstream, radium bioaccumulation is highly probable -but not yet observed- in areas impacted by OGPW disposal. Indeed, radium bioaccumulation in bivalve soft tissue downstream from areas with OGPW disposal remains unstudied. This is concerning as radium has a long biological half-life of documented 10–13 years (Johnston et al., 1984; Ryan et al., 2008) and may be retained even after mussels are purged in clean water (Brenner et al., 2007).

Therefore, the objectives of this study are to determine if in areas historically impacted by Marcellus OGPW, do 1) *Eurynia dilatata* freshwater mussels accumulate and retain radium, and 2) these bivalves retain isotopic and elemental ratio signatures indicative of OGPW.

2. Material and methods

2.1. Site location

The NPDES permitted CWT chosen for this study discharged treated OGPW into the Allegheny River with reported discharges from 2000 to 2019. The Allegheny drainage basin upstream of the location encompasses 5982 $mile^2$ with land use dominated by forest (70.24 %) and hay and pastures fields (12.42 %) (National Land Cover Database); however, the water quality is heavily impacted by French Creek, an upstream tributary, with limited mixing occurring upstream of this outfall location (Brancato and Spear, 2018). Compared to similar facilities along the Allegheny drainage basin, this CWT accepted the most unconventional OGPW (Van Sice et al., 2018) receiving over 500 million liters from 2008 to 2011 (PADEP, 2023). The increased sedimentation and elevated radioactivity measurements near the discharge pipe, resulting in twenty times higher than background count rates, lead to a remediation effort in 2015. Remediation removed the top 30 cm of sediment within 20 m of the outfall- these areas corresponded to locations above the DEP's acceptance criteria of 5 pCi/g combined radium ($^{226}Ra + {}^{228}Ra$) above background (Integrated Environmental Management, 2014; Plexus Scientific Corporation, 2016). The high conductivity plume negatively impacted aquatic wildlife and motivated an aquatic biology investigation lead by the PA Department of Environmental Protection (Brancato and Spear, 2016). The plume extended over 1 km downstream of the outfall and the investigation discovered missing mussel populations up to 400 m downstream with the biggest impact near the outfall. A post-remediation survey was completed in 2016 and confirmed radioactivity levels were below the DEP's acceptance criteria with background conditions defined at 2 pCi/g combined radium. After remediation efforts, the CWT continued conventional OGPW discharges until the facility was fully decommissioned in December 2019.

2.2. Field methods

Ten *E. dilatata* freshwater mussels were collected from the substrate at each sample location with guidance from Pennsylvania Department of Environmental Protection (PADEP) biologists under scientific collector's permits during two sampling events. Samples collected 1 and 2 km upstream of the impacted zone (A; A') are meant to represent background conditions, while samples collected at the outfall (B), 0.5 km downstream (C), and 5 km downstream (D) represent impacted zones (Fig. 1). A subset of ten freshwater mussels were randomly selected from survey bags collected along stream transects from the center to left descending bank at each sample location with a 30-m longitudinal range. All mussels sampled were relatively similar in age/size ranging from 8 to 12 years old with the exception of the outfall location (B). These mussels likely naturalized the area after the sediment remediation efforts and averaged 4–5 years in age. Initial sampling occurred in summer of 2020 with additional (locations A; D) sampling in summer of 2022 to include samples much further downstream; both sampling events occurred after facility discharges had fully ceased. After collection, mussels were frozen (−80 °C) until further analysis. One 500 mL composite sediment grab sample was collected by combining a minimum of 3 subsamples within transects corresponding to the mussels' habitats. Sediment samples were transported in a cooler and refrigerated until further analysis.

2.3. Radium analysis

Radium analysis was performed on soft tissue, hard shell and sediment. Measurements of freshwater mussels include wet mass, length, height, and width dimensions. Mussel samples were partially defrosted to allow for dissection of the inner soft tissue. Mussel soft tissue was rinsed with ultrapure water, separated from the hard shell, and immediately freeze dried. Samples were then pulverized and homogenized using a food processor. For hard shells, one half shell from each sample was cleansed with a sponge and detergent soap to clean off outer debris and rinsed with ultrapure water, dried and then pulverized to a fine powder in a ball mill for 15 min. Sediment samples in triplicate were dried at 105 °C for 24 h, homogenized with a mortar and pestle, and sieved to 1.18 mm. All radium samples were transferred, sealed, and incubated in 24 mL HDPE liquid scintillation vials for 21 days to allow radium daughter products to reach secular equilibrium before analysis.

Radium activities were measured using a Canberra small anode germanium detector (SAGe) gamma spectrometer via the ^{214}Pb, ^{214}Bi, and ^{212}Pb daughter products using the (295, 351, 609) and (239) keV peaks respectively for ^{226}Ra and ^{228}Ra. Activity units are presented in pCi/g to match Pennsylvania reporting limits; however, Bq/g units are supplemented in all tables. Peak counts were only included for samples with counting errors <10 %. ^{212}Pb was used as a proxy for ^{228}Ra sediment activities with the assumption that ^{228}Th, which has a half-life of 1.9 yrs., has reached secular equilibrium. $^{228}Th/^{228}Ra$ ratios in environmental sediment samples indicate approximate secular equilibrium supporting this assumption (Casella et al., 1982; Sheppard et al., 2008). While alpha recoil is less likely to discharge ^{228}Ra from the crystalline hard shell structure, it is possible for this to occur in the soft tissue along with preferential uptake based on bioavailability similar to plant tissue examples (Sheppard et al., 2008). Therefore, this assumption cannot be made for biological samples collected <10 years post discharge. Nevertheless, even with an overestimation, ^{228}Th may still act as a good proxy for relative abundance of ^{228}Ra between site locations. Subsequent tables will report all ^{228}Th and ^{228}Ra interchangeably with this distinction. Minimum detectable activities (MDA) were calculated (Eq. (1)) for select biological samples to confirm detection limits of samples with shell or tissue matrices using the following equation:

$$MDA = \frac{2.71 + 3.29\sqrt{B\left(1 + \frac{n}{2c}\right)}}{m^{*}LT^{*}\varepsilon.} \quad (1)$$

with B background counts, n sample counts, c sample channels per peak, m sample mass, LT sample run period, and ε sample efficiency. Sample

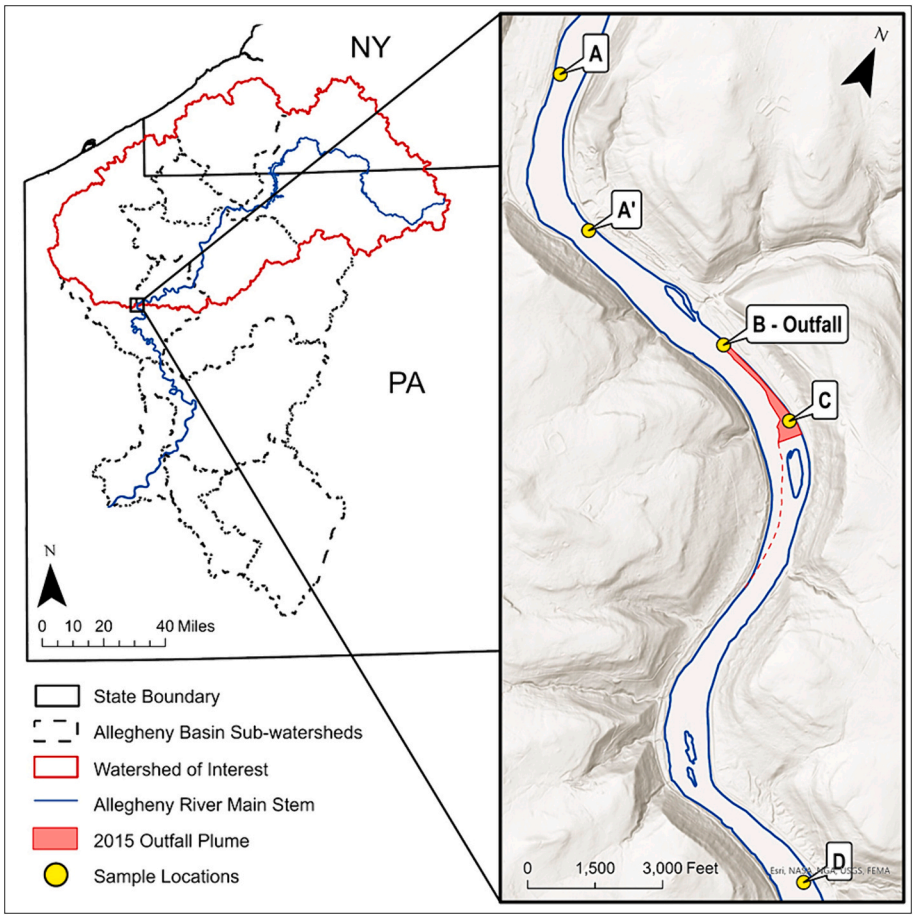

Fig. 1. Map of field sample locations within the Allegheny River Basin with samples collected 1 and 2 km upstream of the facility outfall (A/A'), at the outfall (B), 0.5 km downstream within the discharge plume (C), and 5 km downstream (D) after assumed complete mixing. Plume delineations were done via conductivity breakpoints via the 2016 PADEP Fluid Recovery Services, LLC (FRS) Survey Report.

efficiency was determined using sediment standards at different heights (1 cm, 2 cm, 3.5 cm, and 5 cm) to generate regressions based on sample height corresponding to mass of sample in the 24 mL HDPE liquid scintillation vial. UTS-2 certified uranium tailing sample prepared by Canadian Certified Reference Materials Project (CCRMP) was used to calibrate radium activities and efficiency.

2.4. Cation and strontium isotope analysis

Three soft tissue and hard shell samples from each location were digested following the EPA 3052 method for organically based matrices (EPA METHOD 3052, 1996). Approximately 0.25 g of each sample was digested in 9 mL 2 N distilled nitric acid using a CEM Mars 6 microwave digestion system. 5 mL of 2 N distilled nitric acid was added to soft tissue samples and rerun to allow for complete digestion. Samples were filtered to 0.45 μm and diluted with 2 % distilled nitric acid for cation analysis on a Thermo iCAP 7400 inductively coupled plasma emission spectrometer (ICP-OES) at the Penn State LIME laboratory.

One digested soft tissue and hard shell mussel sample at each site was randomly selected and evaluated for $^{87}Sr/^{86}Sr$ ratios. $^{87}Sr/^{86}Sr$ ratios were measured using a Thermal Ionization Mass Spectrometer (TIMS) at the Penn State LIME laboratory. All measured $^{87}Sr/^{86}Sr$ ratios were corrected for instrumental mass bias using an exponential law applied to measurements of $^{86}Sr/^{88}Sr$ with an assumed true ratio of 0.1194.

2.5. Statistical analysis

A Wilcoxon/Kruskal-Wallis Rank Sums test was run via JMP Pro 17 between site locations with a minimum of 5 samples to determine statistical differences between ^{226}Ra and ^{228}Ra activities in the soft tissue, hard shell, and sediment. Nonparametric comparisons for each pair were done using the Wilcoxon method with a 95 % confidence interval to determine statistical differences between sample locations. All linear regressions were completed in JMP Pro 17 utilizing the Fit function with 95 % confidence intervals.

3. Results and discussion

3.1. Sediment

Combined radium activities ($^{226}Ra + {}^{228}Ra$) in sediment collected upstream of the discharge location (samples A and A') averaged 0.91 ± 0.09 pCi/g and are consistent with background radium activities reported in other studies (0.486–2.135 pCi/g) (Lauer et al., 2018; Warner et al., 2013). The only sample location from this study with elevated radium activities was location C, located 0.5 km downstream of the discharge (mean = 1.45 ± 0.19 pCi/g). There was a significant difference in ^{226}Ra activities in the sediment collected 0.5 km downstream (within the delineated discharge plume) from all other sample locations. All peaks (295, 351, 609) were utilized for this ^{226}Ra analysis resulting in a sample size $n = 9$ per location when including sample triplicates. ^{228}Ra statistical differences were not applicable from one peak measurement as nonparametric comparisons for each pair using the Wilcoxon method recommends a sample size of five or more; however, both ^{228}Ra and ^{226}Ra had the highest reported values 0.5 km downstream. In contrast to previous studies, the sediment sampled at the outfall

contained radium activities similar to background, most likely a result of remediation efforts in 2016. However, consistent with those studies is that sediment outside of the remediation zone farther downstream showed a significant increase in total radium activities. Importantly, $^{228}Ra/^{226}Ra$ at both 0.5 km and 5 km downstream were lower than upstream background levels. The increase in combined radium 0.5 km downstream and the difference in $^{228}Ra/^{226}Ra$ support previous studies that showed increased sediment radium activities downstream of OGPW outfalls (Lauer et al., 2018; McDevitt et al., 2019; Van Sice et al., 2018; Warner et al., 2013) sometimes at distances >1 km. The combination of stream sediment removal during remediation and the time since OGPW discharge (~1 year) led to transport and dilution of impacted sediment farther downstream with little to no elevated radium exposure in the remediation zone.

3.2. Soft tissue radium

Samples collected at two locations (A and A') were combined to represent background, upstream, conditions ($n = 18$; combined radium mean = 1.27 ± 0.24 pCi/g). Mussel soft tissue collected within the discharge plume (0.5 km downstream) retained significantly higher ($p < 0.05$) combined radium activities (mean = 3.44 ± 0.95 pCi/g) compared to background levels. Samples collected in the remediated outfall zone (mean = 1.49 ± 0.38 pCi/g) and 5 km downstream (mean = 1.54 ± 0.33 pCi/g) were not higher with statistical significance. Whether combined or individually ^{226}Ra and ^{228}Ra activities 0.5 km downstream of the outfall also displayed a significant difference from all other sample locations (Fig. 2). A significant difference in the $^{228}Ra/^{226}Ra$ ratio was observed only 5 km downstream of the outfall when compared to upstream conditions. Nevertheless, increased radioactivity is observed 0.5 km downstream of the initial outfall with minimal sample repetitions ($n = 9$). These results indicate that minimal sampling ($n \leq 10$/site) is necessary in order to obtain meaningful results for mussels impacted by waste streams containing ^{226}Ra and ^{228}Ra.

3.3. Hard shell radium

Hard shell background radium activities (mean = 0.10 ± 0.02 pCi/g) were significantly lower than activities within the discharge plume (0.5 km downstream) (mean = 0.34 ± 0.11 pCi/g) and 5 km downstream (mean = 0.19 ± 0.03 pCi/g). Background samples show consistently low radium activities, whereas, with a randomly distributed subset $n \geq 5$, downstream impacted zones show a significant increase in ^{226}Ra activity up to 5 km downstream. Likewise, a significant decrease in the $^{228}Ra/^{226}Ra$ ratio occurs 0.5 km and 5 km downstream of the outfall. This change in the $^{228}Ra/^{226}Ra$ corresponds to the areas with the highest radioactivity with a significant signature observed in the hard shell compared to the soft tissue. While the radium signature is statistically

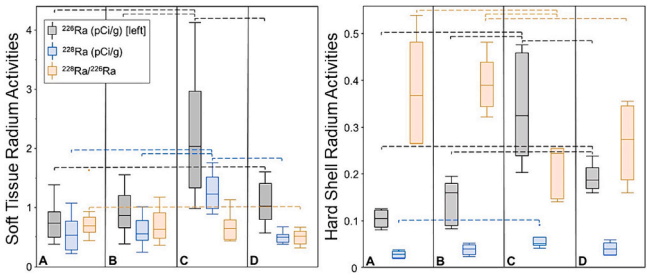

Fig. 2. Soft tissue (left) and shell (right) ^{226}Ra activities, ^{228}Ra activities, and $^{228}Ra/^{226}Ra$ ratios for (A; A') upstream, (B) remediated outfall, (C) 0.5 km downstream, and (D) 5 km downstream locations using a 25-percentile outlier box and whisker plot. Dashed lines represent significant difference between pairs using the Wilcoxon nonparametric comparisons for each pair in JMP Pro 17.

stronger in the hard shell, it is important to note that the measured activities are much lower than what can accumulate in the soft tissue. Individual activity measurements and statistical parameters can be found in the Supplementary Materials. Statistically significant differences between pairs are shown in Fig. 2 represented via dashed lines.

Elevated radium activities and lower $^{228}Ra/^{226}Ra$ ratios are expected in the zones impacted by OGPW within this region. Older discharges of OGPW with unsupported ^{228}Ra and ^{226}Ra will lead to lower $^{228}Ra/^{226}Ra$ ratios over time because of the shorter half-life of ^{228}Ra (5.8 years) compared to ^{226}Ra (1600 years). Unconventional Marcellus OGPW contains elevated ^{226}Ra and would likewise lead to a lower $^{228}Ra/^{226}Ra$. For mussels, the highest risk of exposure and uptake of discharged radium lies within the plume discharge area where increased radium activities in sediment are observed. Our results demonstrate that radium sourced from the outfall of treated OGPW was retained in both soft tissue and hard shell even after the facility was decommissioned and 9 years after peak unconventional OGPW discharge. While the ultimate source of the elevated radium in mussels is the discharge of treated OGPW, it is not clear if the mussels were directly exposed to dissolved radium or radium that was retained in sediment. Evidence suggests that sediment acts as a long-term radium source. The legacy radium retained in sediment is typically in the form of radiobarite but could also be sorbed to iron and manganese oxides (Van Sice et al., 2018). In both scenarios the radium would be bioavailable to mussels despite improvements in water quality and decommissioning of the facility.

Alternatively, mussels are known to retain radium after exposure, even if they are introduced to radium-free water (Brenner et al., 2007). Therefore, it's possible that the radium may have been sourced from direct exposure to OGPW discharges that contained dissolved radium. Once incorporated in the soft tissue the radium is thought to be stored as a radium phosphate (Bollhöfer et al., 2011; Jeffree and Simpson, 1984). The latter may be plausible as mussels grow extensively in their younger years, with much smaller growth rates in terms of overall mass in later years. Mussels collected in 2020 with an average size and estimated age of 8 to 12 years would have been exposed during periods of time with maximum growth to higher activities of radium in sediment when the facility was operating. We did not observe increased radioactivity or changes in the $^{228}Ra/^{226}Ra$ ratio in younger mussel (4–5 years) samples collected near the remediated outfall location. The younger age of the mussels and the remediation of the sediment at the point of discharge confound these variables making it difficult to confirm if radium has been retained in older samples from past exposures. Radium activity along the axis of the shell could help indicate if the radium was incorporated years ago during direct exposure or if the sediment continues to be a source of radium exposure. Previous studies have shown that laser ablation along with age dating on the shell can provide temporal results as the mussel is developing (Geeza et al., 2018b); however, the bulk shell method used in the current study still provides meaningful time averaged results for radium accumulation. The mass of shell necessary for accurate radium analysis (≥ 1 g) limits the use of laser ablation in this instance; however, it may be applied for other metals of interest.

3.4. Metal/Ca

Metal/Calcium ratios in both hard shell and soft tissue were calculated for twelve metals (Table 3). Metal concentrations were normalized to calcium (Ca) because mussels continuously intake and store Ca for biological processes. Normalization helps to identify selective intake and accumulation of other relevant metals as well as to account for potential biomineralization of metals. Sr, Ba, Mg, and Mn concentrations, ratios relative to calcium, and non-thermodynamic partitioning coefficients (D_{Me}) are compared to previously published data expanded from (Geeza et al., 2018a) (Table 1). Hard shell Sr/Ca (0.44–1.33), Ba/Ca (0.08–0.12) and Mn/Ca (0.98–1.24) values in mmol/mol were consistent with previous works, while Mg/Ca (0.16–2.88) values were slightly elevated compared to other environmental samples (Geeza,

Table 1
Sr, Ba, Mg, and Mn concentrations, ratios relative to calcium, and non-thermodynamic partitioning coefficients (D_{Me}) are compared to previously published data expanded from (Geeza et al., 2018a).

Reference (Shells)	Sr (mg/kg)	Sr/Ca (mmol/mol)	D_{Sr}	Ba (mg/kg)	Ba/Ca (mmol/mol)	D_{Ba}	Mg (mg/kg)	Mg/Ca (mmol/mol)	D_{Mg}	Mn (mg/kg)	Mn/Ca (mmol/mol)	D_{Mn}
Faure et al. (1967)			0.22–0.28									
Nyström et al. (1996)	300–600									10–600		
Mutvei and Westermark (2001)										400–6000		
Markich et al. (2002)										300–1700		0.6
Verdegaal (2002)	120–220					0.1				100–700		0.5
Bailey and Lear (2006)	700–1000		0.28									
Langlet et al. (2007)										100–1000		
Ravera et al. (2007)										200–800		
Carroll and Romanek (2008) (Izumida et al., 2011)	120–2000		0.17, 0.26	60–400		0.05	150–500		0.00030–0.00042	80–1700		0.2, 0.5
Zhao et al. (2017)										1130–1380		
Geeza et al. (2018a)	820–3343	1.22–3.82	0.16–0.20	15–270	0.011–0.216	0.11–0.14	26–1200	0.16–0.79	0.0003–0.0008	120–1250	0.16–2.33	32–42
Geeza et al. (2018b) (Avg / location)		0.25–0.52										
Geeza Dissertation (2018)	377–1053		0.16–0.20		0.028–0.045	0.020–0.037		0.15–0.22	0.00052–0.00074		0.43–1.43	0.28–4.47
This Study	460–1360	0.44–1.33	0.08–0.12	112–190	0.08–0.12	0.11–0.19	44–876	0.16–2.88	0.00056–0.0076	602–836	0.98–1.24	0.94–1.28
Reference (Tissue)	**Sr (mg/kg)**	**Sr/Ca (mmol/mol)**	**D_{Sr}**	**Ba (mg/kg)**	**Ba/Ca (mmol/mol)**	**D_{Ba}**	**Mg (mg/kg)**	**Mg/Ca (mmol/mol)**	**D_{Mg}**	**Mn (mg/kg)**	**Mn/Ca (mmol/mol)**	**D_{Mn}**
McDevitt et al. (2021)		4.07–28.13			4.92–11.56			41–104			272–384	
Piotrowski et al. (2020)	427–2308	5–27	0.27–4.84	93–5705	0.7–30.6	1.66–5.34	544–836	23–43	0.03–0.11	18,564–23,524	243–348	
This Study	65–841	1.17–4.98		99–2282	1.9–11		1129–2729	58–123		965–10,772	46–128	

2018; Geeza et al., 2018a). A strong linear relationship was defined between the K/Ca, Mg/Ca, and Na/Ca ratios relative to distance from the outfall for samples collected 1 km upstream, at the outfall, and 0.5 km downstream (Fig. 3). The linear correlation is not significant when including the location 5 km downstream. However, the metal/calcium ratios 5 km downstream are significantly below background levels. Other metal/Ca ratio (e.g. Ba, Mn, Sr, and Ra) correlations were weak.

Dissolved Mg, Na and Ca concentrations for areas of the Allegheny River near the discharge were reported in the 2016 PADEP Fluid Recovery Services, LLC (FRS) Survey Report (Brancato and Spear, 2016). These values were converted to molar concentrations and then used to create a regression between metal/Ca molar ratios observed in Allegheny water and in the hard shell (Fig. 4). D_{Me} values were calculated (Eq. (2)) using this water chemistry. D_{Ba} (0.11–0.19), D_{Mg} (0.00056–0.00076) and D_{Mn} (0.94–1.28) partitioning coefficients aligned with previous environmental samples, while D_{Sr} (0.08–0.12) was slightly lower (Table 1).

$$D_{Me} = \frac{\frac{c_{Me,shell}}{c_{Ca,shell}}}{\frac{c_{Me,water}}{c_{Ca,water}}} \quad (2)$$

The results indicate that the shell Mg/Ca and Na/Ca ratios correspond to the water metal/calcium ratios during a time of active discharge. Na/Ca ratios negatively correlate while Mg/Ca positively correlate with ratios recorded in the shells.

Soft tissue metal/Ca ratios of interest included strontium (Sr) and lead (Pb). Sr/Ca (mean = 3.20 ± 0.98 mmol/mol) and Pb/Ca (5.18 ± 1.61 mmol/cmol) ratios in the soft tissue were elevated at the remediated discharge compared to upstream (1.71 ± 0.10; 2.36 ± 0.18). respectively. Compared to previous environmental samples, Sr/Ca ratios measured in this study were slightly lower than reported values (4.07–28.13 mmol/mol) (McDevitt et al., 2021; Piotrowski et al., 2020). Pb was below the detection limit in the hard shell; however, shell Sr/Ca showed a similar trend with values at the discharge averaging 0.94 mmol/mol compared to upstream (0.55) (Table 2).

Decreased K/Ca, Na/Ca, and Mg/Ca observed in mussel shell collected from impacted zones could be attributed to the significant increase in available dissolved Ca^{2+} downstream of the facility discharge. OGPW contains Ca^{2+} well above seawater concentrations leading to elevated concentrations of Ca^{2+} in the Allegheny downstream of OGPW discharges. The 2016 PADEP Fluid Recovery Services, LLC (FRS) Survey Report reported a concentration of 6680 mg/L at the discharge, over 300 times the concentration upstream (18.1 mg/L) (Brancato and Spear, 2016). Previous work on Australian freshwater mussels, showed a decrease in radium uptake with increased calcium concentrations (Bollhöfer et al., 2011; Doering and Bollhöfer, 2017). Our results observe this phenomenon with metals (K, Mg, and Na); however, we see the opposite trend with strontium, radium, and lead. These metals actually increase relative to calcium 0.5 km downstream, the location of highest observed impact from discharges.

3.5. Strontium isotopic analysis

Compared to background levels, $^{87}Sr/^{86}Sr$ isotopic ratios showed a declining trend from the outfall in both the soft tissue and hard shell (Table 3). Shell and tissue $^{87}Sr/^{86}Sr$ ratios in impacted zones of this study (0.711330–0.712349) at 0.5 km and 5 km downstream are closest to Marcellus OGPW ($^{87}Sr/^{86}Sr$ = 0.7106) (Chapman et al., 2012) compared to background values (0.712561–0.712902) collected 1–2 km upstream of the discharge (Table 3). Background hard shell samples collected ~150 km upstream of this site recorded an average $^{87}Sr/^{86}Sr$ ratio of 0.7140 (Geeza et al., 2018b) and likely represent expected values of the Allegheny before the influence of any OGPW.

If the strontium signature observed in the shells 5 km downstream was sourced from disposal of Marcellus OGPW a simple mixing model could elucidate the percentage of OGPW incorporated into the shell.

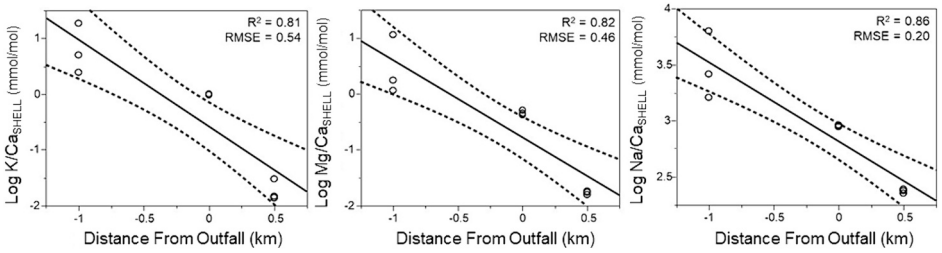

Fig. 3. Linear regressions for measured metal/calcium ratios (K/Ca, Mg/Ca, and Na/Ca) in hard shell samples relative to sample locations (A', B, and C) in km. A strong relationship is defined for these three metals of interest.

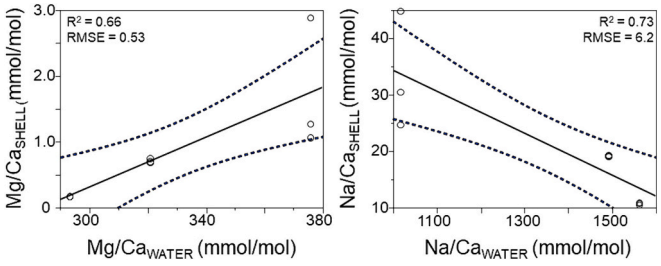

Fig. 4. Shell metal/Ca ratios relative to water metal/Ca ratios at sample locations (A', B, and C) collected from the 2016 PADEP Fluid Recovery Services, LLC (FRS) Survey Report (Brancato and Spear, 2016).

Table 2
Freshwater mussel soft tissue and hard shell Sr/Ca and Pb/Ca sampled at field locations (A') upstream, (B) remediated outfall, (C) 0.5 km downstream, and (D) 5 km downstream.

Soft Tissue	Sr/Ca (mmol/mol)	Pb/Ca (mmol/cmol)	Hard Shell	Sr/Ca (mmol/mol)
A' – 1	1.94	2.74	A' – 1	0.45
A' – 2	1.70	2.48	A' – 2	0.51
A' – 3	1.36	1.86	A' – 3	0.68
B – 1	2.43	2.58	B – 1	0.50
B – 2	1.18	2.94	B – 2	0.63
B – 3	1.65	1.79	B – 3	0.53
C – 1	2.53	3.00	C – 1	1.34
C – 2	5.00	8.02	C – 2	0.76
C – 3	2.10	4.53	C – 3	0.72
D – 1	2.52	<DL	D – 1	N/A
D – 2	2.50	<DL	D – 2	0.58
D – 3	2.55	<DL	D – 3	N/A

Here we used upstream Allegheny River water (Sr = 50 μg/L and plume concentrations (Sr = 201 μg/L) reported in the FRS report as endmembers. We measured background values of $^{87}Sr/^{86}Sr$ = 0.71256 1 km upstream of the facility. Note that these values are remarkably similar to values of $^{87}Sr/^{86}Sr$ in shells ($^{87}Sr/^{86}Sr$ = 0.7125) collected ~150 km upstream the Allegheny in Warren PA. The Warren, PA shells we collected directly downstream of a different OGPW treatment facility and the values reported in (Geeza et al., 2018b). For the plume we used the 25th and 75th quartile values for $^{87}Sr/^{86}Sr$ (0.71071 and 0.71117) of Marcellus OGPW (Tasker et al., 2019) and calculate between 40 and 60 % of the strontium incorporated into the shell could be sourced from Marcellus OGPW.

The changes in hard shell and soft tissue $^{87}Sr/^{86}Sr$ relative to values observed upstream display the influence of OGPW discharges to change water chemistry and isotopic signatures recorded in aquatic life. These results suggest hard shell is a consistent tracer for impacted mussels up to 5 km downstream of OGPW disposals. Interestingly, the $^{87}Sr/^{86}Sr$ measured in our samples collected upstream of the local discharge may be indicative of historical OGPW inputs to the Allegheny that occurred much farther upstream, for example discharges in Warren PA (Geeza et al., 2018b). Because of the relatively low Sr concentrations in the Allegheny River and very high relative values for Sr in OGPW, these historical discharges changed both the concentration and isotopic ratio of the entire Allegheny River.

3.6. Regression analysis

Total radium activities, $^{228}Ra/^{226}Ra$ ratios and $^{87}Sr/^{86}Sr$ isotopic ratios in hard shell and soft tissue were analyzed via regression to assess potential explanatory variables. The factors that were the best predictors were the sediment radium activity and distance from the outfall (Fig. 5). The strongest relationship was found between the total sediment radium activities and the total soft tissue and shell radium activities. Both produced $R^2 = 0.56$ and $P < 0.0001$, with a better root mean squared error in the hard shell (RMSE = 0.07). While not significant, a negative relationship was found between the distance to the outfall and $^{228}Ra/^{226}Ra$ ratios in both hard shell and soft tissue. Lastly, $^{87}Sr/^{86}Sr$ isotopic ratios in the soft tissue produced a strong linear relationship with distance from the outfall location. While this relationship was not apparent in the hard shell, all values decrease relative to background in the areas at the discharge and farther downstream (0.5 and 5 km) (Fig. 5).

Results from this study suggests both soft tissue and hard shell samples may be useful as biological indicators of past OGPW disposals with differences in radium activity, metal/Ca ratios and isotopic ratios ($^{228}Ra/^{226}Ra$ and $^{87}Sr/^{86}Sr$) observed in bulk samples collected and analyzed years after OGPW discharges ceased. On a per-gram basis radium accumulation in mussel tissue samples within the discharge plume area is up to four times higher than measured in sediment and 12 times more than hard shell. This is concerning given the limited research regarding freshwater mussel contaminant uptake creating limitations to fully understand the consequences of radium exposure. Freshwater mussels will retain radioactivity even after being purged in radium-free water (Brenner et al., 2007) leaving a legacy of radium contamination that will last after contaminated sediment has been transported downstream. Radium activities were significantly higher in soft tissue compared to values in sediment and shells, indicating the need for a better understanding of the fate of radium in benthic ecosystems. From a health perspective, increased radium levels in the soft tissue may pose health risks up the trophic food chain, including muskrats who consume large quantities of freshwater mussels and may be at risk for magnified exposure to radium. Muskrats have documented population declines unattributed to natural hunting rates (Ahlers and Heske, 2017). Further research is needed to identify radium in animals that prey on freshwater mussels within these impacted areas.

This study identifies multiple tracers for OGPW disposal impacts including radium bioaccumulation and a suite of elemental/isotopic ratios with minimal sampling repetitions. Freshwater mussel biomonitoring capabilities are still an emerging area of research with limited field replication and the applicability of this method still needs further investigation and spatial repetition.

Table 3
Averaged sediment, tissue, and shell radioactivity, metal/Ca, and strontium isotopic ratio results for field sample locations with samples collected 1 and 2 km upstream of the facility outfall (A/A'), at the outfall (B), 0.5 km downstream within the discharge plume, and 5 km downstream (D).

	UPSTREAM			REMEDIATED DISCHARGE			DOWN 0.5 km			DOWN 5 km		
	N	Average	SD	N	Average	SD	N	Average	SD	N	Average	SD
SEDIMENT												
Radium												
^{226}Ra (pCi/g)	4	0.42	0.02	3	0.49	0.05	3	0.73	0.04	3	0.41	0.04
^{226}Ra (Bq/kg)	4	15.7	0.9	3	18.2	1.7	3	26.9	1.5	3	15.3	1.6
^{228}Ra (pCi/g)	4	0.49	0.03	3	0.45	0.05	3	0.72	0.04	3	0.43	0.08
^{228}Ra (Bq/kg)	4	18.0	1.2	3	18.0	1.8	3	26.7	1.4	3	16.0	3.0
Total Ra (^{226}Ra + ^{228}Ra) (pCi/g)	4	0.91	0.05	3	0.95	0.09	3	1.45	0.08	3	0.85	0.12
^{228}Ra/^{226}Ra (pCi/pCi)	4	1.15	0.02	3	0.92	0.01	3	0.99	0.02	3	1.04	0.09
SOFT TISSUE												
Radium												
^{226}Ra (pCi/g)	18	0.74	0.26	9	0.90	0.34	9	2.19	0.99	8	1.06	0.34
^{226}Ra (Bq/kg)	18	27.2	9.7	9	33.4	12.5	9	81.2	36.6	8	39.0	12.4
^{228}Ra (pCi/g)	18	0.53	0.24	9	0.59	0.22	9	1.25	0.28	8	0.49	0.09
^{228}Ra (Bq/kg)	18	19.7	8.7	9	21.8	8.3	9	46.3	10.5	8	18.0	3.2
Total Ra (^{226}Ra + ^{228}Ra) (pCi/g)	18	1.27	0.47	9	1.49	0.49	9	3.44	1.24	8	1.54	0.39
^{228}Ra/^{226}Ra (pCi/pCi)	18	0.73	0.26	9	0.70	0.25	9	0.65	0.22	8	0.49	0.12
Metal Ratios (mmol/mol)												
Al/Ca	6	16.45	9.69	3	14.91	2.91	3	10.94	3.52	3	7.93	1.23
Ba/Ca	6	5.74	3.41	3	7.01	1.13	3	9.28	0.97	3	7.18	0.94
Cu/Ca	6	0.21	0.05	3	0.21	0.06	3	0.16	0.03	3	0.18	0.04
Fe/Ca	6	56.59	23.21	3	44.46	8.49	3	56.96	1.12	3	44.75	3.45
K/Ca	6	63.20	23.48	3	47.05	7.35	3	43.64	3.04	3	57.48	5.34
Mg/Ca	6	82.76	19.06	3	69.46	7.47	3	63.34	4.89	3	77.71	7.41
Mn/Ca	6	84.84	26.74	3	101.21	19.56	3	119.04	16.89	3	90.78	9.70
Na/Ca	6	152.05	76.29	3	91.78	26.80	3	131.77	52.88	3	174.73	25.59
Pb/Ca	3	0.02	0.0037	3	0.02	0.00	3	0.05	0.02	0	N/A	N/A
Sr/Ca	6	1.71	0.19	3	1.75	0.52	3	3.20	1.27	3	2.52	0.02
Zn/Ca	3	2.99	0.20	3	3.00	0.58	3	2.76	0.55	3	2.68	0.23
Ra/Ca (pCi/mol)	6	7502.19	4385.93	3	3734.91	1869.02	3	2975.92	1363.70	3	4293.94	1624.64
Stable Isotopes												
^{87}Sr/^{86}Sr	1	0.712902 ± 0.0000106		1	0.712511 ± 0.0000113		1	0.712349 ± 0.0000143		1	0.711329 ± 0.0000122	
HARD SHELL												
Radium												
^{226}Ra (pCi/g)	5	0.08	0.01	5	0.10	0.03	6	0.28	0.09	5	0.15	0.02
^{226}Ra (Bq/kg)	5	2.8	0.5	5	3.8	1.2	6	10.4	3.5	5	5.5	0.7
^{228}Ra (pCi/g)	5	0.03	0.01	5	0.04	0.01	6	0.06	0.02	5	0.04	0.01
^{228}Ra (Bq/kg)	5	1.0	0.2	5	1.4	0.4	6	2.1	0.6	5	1.5	0.5
Total Ra (^{226}Ra + ^{228}Ra) (pCi/g)	5	0.10	0.02	5	0.14	0.04	6	0.34	0.11	5	0.19	0.03
^{228}Ra/^{226}Ra (pCi/pCi)	5	0.37	0.10	5	0.39	0.05	6	0.21	0.05	5	0.27	0.07
Metal Ratios (mmol/mol)												
Al/Ca	3	0.13	0.01	3	0.13	0.01	3	0.18	0.03	1	0.17	N/A
Ba/Ca	3	0.09	0.01	3	0.09	0.01	3	0.10	0.02	1	0.09	N/A
Cu/Ca	3	0.0251	0.0019	3	0.0261	0.0026	3	0.0247	0.0004	1	0.0279	N/A
Fe/Ca	3	0.20	0.02	3	0.15	0.02	3	0.24	0.04	1	0.19	N/A
K/Ca	3	2.35	0.88	3	0.99	0.01	3	0.18	0.03	1	0.52	N/A
Mg/Ca	3	1.74	0.81	3	0.71	0.03	3	0.17	0.00	1	0.51	N/A
Mn/Ca	3	1.18	0.05	3	1.11	0.10	3	1.07	0.08	1	1.23	N/A
Na/Ca	3	33.29	8.44	3	19.16	0.12	3	10.69	0.15	1	14.43	N/A
Pb/Ca	0	N/A	N/A	0	N/A	N/A	0	N/A	N/A	0	N/A	N/A
Sr/Ca	3	0.55	0.10	3	0.55	0.05	3	0.94	0.28	1	0.58	N/A
Zn/Ca	3	0.0084	0.0023	3	0.0059	0.0001	3	0.0044	0.0005	1	0.0055	N/A
Ra/Ca (pCi/mol)	3	9.60	0.99	3	14.51	1.34	3	28.57	8.87		20.96	N/A
Stable Isotopes												
^{87}Sr/^{86}Sr	1	0.712563 ± 0.0000107		1	0.711516 ± 0.0000131		1	0.711392 ± 0.0000115		1	0.711658 ± 0.0000093	

3.7. Exposure considerations

While there is no defined reference threshold value for the organism's safety, dose limits set by the US-DOE are 10 mGy d − 1 for aquatic animals with an international recommended limit 400 μGy h − 1 for chronic exposure (Department of Energy, 2019), and a dose rate screening value of 10 μGy h − 1 suggested by ERICA tool (J. E. Brown et al., 2008). These values are generalized and do not consider specific specie and exposure pathways. Mussels filter feed on particulate matter in the benthic ecosystem, so there is the expectation to accumulate more than predicted in these general calculations given the chemical properties of the radium and feeding nature of the mussel. This needs to be properly investigated using similar methods as other studies (Din et al., 2023; Khandaker et al., 2013) utilizing the ERICA tool for organism and site-specific toxicity analysis. Given water effluent ^{226}Ra activities of 11 pCi/L measured in 2015 (Lauer et al., 2018), mollusk dose conversion coefficients for internal exposure (0.017) and a concentration factor of (3) as recommended by (Brown et al., 2003; Pröhl, 2003), we calculate a maximum dose rate of 21 μGy h − 1, which falls below recommended thresholds, but above the ERICA recommended screening value. This value is conservative as it is unweighted for alpha or beta emission and excludes external dose rates. Further research may

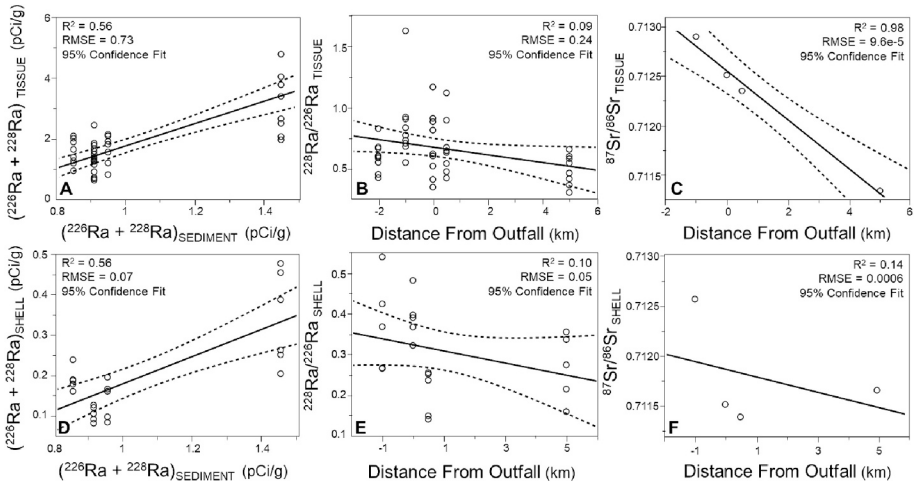

Fig. 5. Regression analysis for tissue total radium activity (A), $^{228}Ra/^{226}Ra$ ratios (B), and $^{87}Sr/^{86}Sr$ ratios (C) and shell total radium activity (D), $^{228}Ra/^{226}Ra$ ratios (E), and $^{87}Sr/^{86}Sr$ ratios (F) relative to total sediment radium or distance from outfall chosen from best fit.

expand on this using ERICA modeling software to properly understand radium toxicity to mussels in OGPW impacted sediment. A larger concern with measured values in this study is biomagnification up the food chain for muskrats and other animals that can consume hundreds of mussels each year. Mussels that previously grew in the outfall zone before remediation of the sediment must have experienced toxic levels of either overall salinity or radium exposures as no mussels were found in the area of active discharge during a 2015 survey (Brancato and Spear, 2016); however, it would be difficult to determine the exact cause of death.

Additionally, while these mussels are not typically harvested for consumption, there are many instances in other regions where mussels (and other bivalves) are harvested, and health risks would be associated with human consumption. Brazil nuts, a food with known active radioactivity exposure monitoring, contain 0.47 μSv to 0.80 μSv in a 28 g serving (Parekh et al., 2008). The maximum value calculated for a single mussel collected in this study is 63.42 μSv using methods outlined by the Food and Agricultural Organization (Food and Agricultural Organization, n.d.). This estimate is much higher than the Brazil nut example; however, both exposure values are only a small fraction of the average dose received annually in the US (~3600 μSv) from all sources of radiation.

4. Conclusion

Historical discharges of high salinity OGPW to surface water have led to legacy radioactivity contamination in the streambed sediment, which created a long-term radium source for organisms such as freshwater mussels. This study is the first to show freshwater mussels, *E. dilatata,* sampled downstream of a legacy OGPW disposal demonstrated significant bioaccumulation of both ^{226}Ra and ^{228}Ra compared to background levels, and bulk tissue and shell measurements can provide meaningful results without the need for exhaustive techniques such as laser ablation. Contaminants associated with OGPW (e.g., Sr, Pb) showed increased concentrations in the soft tissue compared to background as recorded in metal/Ca ratios. Bulk hard shell measurements proved the most consistent for biomonitoring this pollution with multiple signatures indicative of OGPW exposures including changes in isotopic tracers $^{228}Ra/^{226}Ra$ and $^{87}Sr/^{86}Sr$, elemental ratios (K, Mg, and Na/Ca), and radioactivity (^{228}Ra and ^{226}Ra) recorded in hard shell collected up to 5 km downstream of the original outfall location.

CRediT authorship contribution statement

Katharina Pankratz: Writing – original draft, Visualization, Resources, Methodology, Investigation, Formal analysis, Conceptualization. **Nathaniel R. Warner:** Writing – review & editing, Supervision, Resources, Methodology, Funding acquisition, Conceptualization.

Declaration of competing interest

The authors declare the following financial interests/personal relationships which may be considered as potential competing interests: Nathaniel R. Warner reports financial support was provided by National Science Foundation. If there are other authors, they declare that they have no known competing financial interests or personal relationships that could have appeared to influence the work reported in this paper.

Data availability

All data is available in the supplementary materials.

Acknowledgements

The authors would like to acknowledge and thank the PADEP biologists Joseph Brancato, James Grassi, and others who helped sample and accurately identify the freshwater mussels used in this study. This work was supported by the Pennsylvania State University Graduate Fellowship which provided student support and funding by the National Science Foundation [NSF-CAREER-Award #1942601]. The authors would like to thank anonymous reviewers for their valuable input.

Appendix A. Supplementary data

Supplementary data to this article can be found online at https://doi.org/10.1016/j.scitotenv.2024.172151.

References

Ahlers, A.A., Heske, E.J., 2017. Empirical evidence for declines in muskrat populations across the United States. J. Wildl. Manag. 81 (8), 1408–1416. https://doi.org/10.1002/jwmg.21328.

Asikainen, M., 1981. Radium content and the 226Ra/228Ra activity ratio in groundwater from bedrock. Geochim. Cosmochim. Acta 45 (8), 1375–1381. https://doi.org/10.1016/0016-7037(81)90230-1.

Bailey, T.R., Lear, C.H., 2006. Testing the effect of carbonate saturation on the Sr/Ca of biogenic aragonite: a case study from the River Ehen, Cumbria, UK. Geochemistry, Geophys. Geosystems 7 (3).

Barbot, E., Vidic, N.S., Gregory, K.B., Vidic, R.D., 2015. Spatial and temporal correlation of water quality parameters of produced waters from Devonian-age shale following hydraulic fracturing. Wastewater and Shale Formation Development: Risks, Mitigation, and Regulation 41–59. https://doi.org/10.1201/b18648-5.
Barker, F.B., Thatcher, L.L., 1957. Modified determination of radium in water. Anal. Chem. 29 (11), 1573–1575. https://doi.org/10.1021/ac60131a003.
Bollhöfer, A., Brazier, J., Humphrey, C., Ryan, B., Esparon, A., 2011. A study of radium bioaccumulation in freshwater mussels, Velesunio angasi, in the Magela Creek catchment, Northern Territory, Australia. J. Environ. Radioactivity 102 (10), 964–974. https://doi.org/10.1016/j.jenvrad.2010.04.001.
Brancato, J., Spear, R., 2016. PA Department of Environmental Protection FRS Survey Report. PA Department of Environmental Protection.
Brancato, J., Spear, R., 2018. PA Department of Environmental Protection STP Survey Report.
Brenner, M., Smoak, J.M., Leeper, D.A., Streubert, M., Baker, S.M., 2007. Radium-226 accumulation in Florida freshwater mussels. Limnol. Oceanogr. 52 (4), 1614–1623. https://doi.org/10.4319/lo.2007.52.4.1614.
Brown, J., Hosseini, A., Børretzen, P., 2003. Framework for Assessment of Environmental Impact Deliverable 5 Handbook for Assessment of the Exposure of Biota to Ionising Radiation from Radionuclides in the Environment.
Brown, J.E., Alfonso, B., Avila, R., Beresford, N.A., Copplestone, D., Pröhl, G., Ulanovsky, A., 2008. The ERICA tool. J. Environ. Radioact. 99 (9), 1371–1383. https://doi.org/10.1016/j.jenvrad.2008.01.008.
Burgos, W.D., Castillo-Meza, L., Tasker, T.L., Geeza, T.J., Drohan, P.J., Liu, X., Landis, J. D., Blotevogel, J., McLaughlin, M., Borch, T., Warner, N.R., 2017. Watershed-scale impacts from surface water disposal of oil and gas wastewater in Western Pennsylvania. Environ. Sci. Tech. 51 (15), 8851–8860. https://doi.org/10.1021/acs.est.7b01696.
Carroll, M., Romanek, C.S., 2008. Shell layer variation in trace element concentration for the freshwater bivalve Elliptio complanata. Geo-Mar. Lett. 28 (5–6), 369–381. https://doi.org/10.1007/s00367-008-0117-3.
Casella, V.R., Fleissner, J.G., Styron, C.E., 1982. Secular Equilibrium of Radium in Western Coal, pp. 473–479. https://doi.org/10.1007/978-1-4684-4133-8_32.
Chapman, E.C., Capo, R.C., Stewart, B.W., Kirby, C.S., Hammack, R.W., Schroeder, K.T., Edenborn, H.M., 2012. Geochemical and strontium isotope characterization of produced waters from marcellus shale natural gas extraction. Environ. Sci. Tech. 46 (6), 3545–3553. https://doi.org/10.1021/es204005g.
Chapman, E.C., Capo, R.C., Stewart, B.W., Hedin, R.S., Weaver, T.J., Edenborn, H.M., 2013. Strontium isotope quantification of siderite, brine and acid mine drainage contributions to abandoned gas well discharges in the Appalachian plateau. Appl. Geochem. 31, 109–118. https://doi.org/10.1016/j.apgeochem.2012.12.011.
Dailianis, S., 2011. Environmental impact of anthropogenic activities: The use of mussels as a reliable tool for monitoring marine pollution. In: Mussels: Anatomy, Habitat and Environmental Impact, pp. 43–72.
Department of Energy, 2019. A Graded Approach for Evaluating Radiation Doses to Aquatic and Terrestrial Biota.
Din, K.S., Ahmed, N.K., Abbady, A., Abdallah, F.M., 2023. Exposure of aquatic organisms to natural radionuclides in irrigation drains, Qena, Egypt. Scientific Reports 13 (1). https://doi.org/10.1038/s41598-023-27594-4.
Doering, C., Bollhöfer, A., 2017. Water hardness determines 226Ra uptake in the tropical freshwater mussel. J. Environ. Radioact. 172, 96–105. https://doi.org/10.1016/j.jenvrad.2017.03.019.
Dresel, P.E., Rose, A.W., Rendell, E.G., Quigley, J., Dunn, C.A., Love, G.E.W., 2010. Chemistry and Origin of Oil and Gas Well Brines in Western Pennsylvania.
EPA METHOD 3052, 1996. Microwave Assisted Acid Digestion of Siliceous and Organically Based Matrices.
Faure, G., Crocket, J.H., Hueley, P.M., 1967. Some aspects of the geochemistry of strontium and calcium in the Hudson Bay and the Great Lakes. Geochim. Cosmochim. Acta 31 (3), 451–461. https://doi.org/10.1016/0016-7037(67)90053-1.
Ferrar, K.J., Michanowicz, D.R., Christen, C.L., Mulcahy, N., Malone, S.L., Sharma, R.K., 2013. Assessment of effluent contaminants from three facilities discharging marcellus shale wastewater to surface waters in Pennsylvania. Environ. Sci. Tech. 47 (7), 3472–3481. https://doi.org/10.1021/es301411q.
Food and Agricultural Organization, F. (n.d.). Codex General Standard for Contaminants and Toxins in Food and Feed (Codex Stan 193–1995).
Geeza, T.J., 2018. Mussels of the Family Unionidae as Bio-Monitors of Surface Water Quality (Issue December). The Pennsylvania State University.
Geeza, T.J., Gillikin, D.P., Goodwin, D.H., Evans, S.D., Watters, T., Warner, N.R., 2018a. Controls on magnesium, manganese, strontium, and barium concentrations recorded in freshwater mussel shells from Ohio. Chem. Geol. 526 (December 2017), 142–152. https://doi.org/10.1016/j.chemgeo.2018.01.001.
Geeza, T.J., Gillikin, D.P., McDevitt, B., Van Sice, K., Warner, N.R., 2018b. Accumulation of Marcellus formation oil and gas wastewater metals in freshwater mussel shells [research-article]. Environ. Sci. Tech. 52 (18), 10883–10892. https://doi.org/10.1021/acs.est.8b02727.
Gonneea, M.E., Morris, P.J., Dulaiova, H., Charette, M.A., 2008. New perspectives on radium behavior within a subterranean estuary. Mar. Chem. 109 (3–4), 250–267. https://doi.org/10.1016/j.marchem.2007.12.002.
Gustafson, L., Showers, W., Kwak, T., Levine, J., Stoskopf, M., 2007. Temporal and spatial variability in stable isotope compositions of a freshwater mussel: implications for biomonitoring and ecological studies. Oecologia 152 (1), 140–150. https://doi.org/10.1007/s00442-006-0633-7.
Haluszczak, L.O., Rose, A.W., Kump, L.R., 2013. Geochemical evaluation of flowback brine from Marcellus gas wells in Pennsylvania, USA. Appl. Geochem. 28, 55–61. https://doi.org/10.1016/j.apgeochem.2012.10.002.
Integrated Environmental Management, Inc., 2014. Remediation Plan for the Franklin Site Report No. 2013013/G-5490 (Rev. 1) Part 1.
Ismail, N.S., Müller, C.E., Morgan, R.R., Luthy, R.G., 2014. Uptake of contaminants of emerging concern by the bivalves anodonta californiensis and corbicula fluminea. Environ. Sci. Tech. 48 (16), 9211–9219. https://doi.org/10.1021/es5011576.
Izumida, H., Yoshimura, T., Suzuki, A., Nakashima, R., Ishimura, T., Yasuhara, M., Inamura, A., Shikazono, N., Kawahata, H., 2011. Biological and water chemistry controls on Sr/Ca, Ba/Ca, Mg/Ca and δ18O profiles in freshwater pearl mussel Hyriopsis sp. Palaeogeogr. Palaeoclimatol. Palaeoecol. 309 (3–4), 298–308. https://doi.org/10.1016/j.palaeo.2011.06.014.
Jeffree, R.A., Simpson, R.D., 1984. Radium-226 is accumulated in calcium granules in the tissues of the freshwater mussel, velesunio angasi: support for a metabolic analogue hypothesis? Comparative Biochemistry and Physiology – Part A: Physiology 79 (1), 61–72. https://doi.org/10.1016/0300-9629(84)90708-4.
Johnston .M.,.A., A., Marten, R., Martin, P., Pettersson, H., 1984. Uranium Series Radionuclide Concentrations in Significant Aboriginal Foods. In: Alligators Rivers Region Research Institute Report.
Khandaker, M.U., Wahib, N.B., Amin, Y.M., Bradley, D.A., 2013. Committed effective dose from naturally occuring radionuclides in shellfish. Radiat. Phys. Chem. 88, 1–6. https://doi.org/10.1016/j.radphyschem.2013.02.034.
Kolesar Kohl, C.A., Capo, R.C., Stewart, B.W., Wall, A.J., Schroeder, K.T., Hammack, R. W., Guthrie, G.D., 2014. Strontium isotopes test long-term zonal isolation of injected and Marcellus formation water after hydraulic fracturing. Environ. Sci. Tech. 48 (16), 9867–9873. https://doi.org/10.1021/es501099k.
Landis, J.D., Sharma, M., Renock, D., 2018a. Rapid desorption of radium isotopes from black shale during hydraulic fracturing. 2. A model reconciling radium extraction with Marcellus wastewater production. Chem. Geol. 500 (August), 194–206. https://doi.org/10.1016/j.chemgeo.2018.08.001.
Landis, J.D., Sharma, M., Renock, D., Niu, D., 2018b. Rapid desorption of radium isotopes from black shale during hydraulic fracturing. 1. Source phases that control the release of Ra from Marcellus shale. Chem. Geol. 496 (August), 1–13. https://doi.org/10.1016/j.chemgeo.2018.06.013.
Langlet, D., Alleman, L.Y., Plisnier, P.D., Hughes, H., André, L., 2007. Manganese content records seasonal upwelling in Lake Tanganyika mussels. Biogeosciences 4 (2), 195–203. https://doi.org/10.5194/bg-4-195-2007.
Lauer, N.E., Warner, N.R., Vengosh, A., 2018. Sources of radium accumulation in stream sediments near disposal sites in Pennsylvania: implications for disposal of conventional oil and gas wastewater. Environ. Sci. Tech. 52 (3), 955–962. https://doi.org/10.1021/acs.est.7b04952.
Markich, S.J., Jeffree, R.A., Burke, P.T., 2002. Freshwater bivalve shells as archival indicators of metal pollution from a copper-uranium mine in tropical northern Australia. Environ. Sci. Technol. 36 (5), 821–832. https://doi.org/10.1021/es011066c.
McDevitt, B., McLaughlin, M., Cravotta, C.A., Ajemigbitse, M.A., Van Sice, K.J., Blotevogel, J., Borch, T., Warner, N.R., 2019. Emerging investigator series: radium accumulation in carbonate river sediments at oil and gas produced water discharges: implications for beneficial use as disposal management. Environmental Science: Processes and Impacts 21 (2), 324–338. https://doi.org/10.1039/c8em00336j.
McDevitt, B., McLaughlin, M.C., Vinson, D.S., Geeza, T.J., Blotevogel, J., Borch, T., Warner, N.R., 2020. Isotopic and element ratios fingerprint salinization impact from beneficial use of oil and gas produced water in the Western U.S. Sci. Total Environ. 716, 137006 https://doi.org/10.1016/j.scitotenv.2020.137006.
McDevitt, B., Geeza, T.J., Gillikin, D.P., Warner, N.R., 2021. Freshwater mussel soft tissue incorporates strontium isotopic signatures of oil and gas produced water. ACS ES&T Water 1 (9), 2046–2056. https://doi.org/10.1021/acsestwater.1c00135.
Merschel, G., Bau, M., 2015. Rare earth elements in the aragonitic shell of freshwater mussel Corbicula fluminea and the bioavailability of anthropogenic lanthanum, samarium and gadolinium in river water. Sci. Total Environ. 533, 91–101. https://doi.org/10.1016/j.scitotenv.2015.06.042.
Metcalfe, J.L., Charlton, M.N., 1990. Freshwater Mussels as Biomonitors for Organic Industrial Contaminants and Pesticides in the St. Lawrence River. In: Thee Science of the Total Environment, pp. 595–615.
Mutvei, H., Westermark, T., 2001. How Environmental Information Can Be Obtained from Naiad Shells. Ecology and Evolution of the Freshwater Mussels Unionoida 145, 367–379. https://doi.org/10.1007/978-3-642-56869-5_21.
Nelson, A.W., Eitrheim, E.S., Knight, A.W., May, D., Mehrhoff, M.A., Shannon, R., 2015. Understanding the Radioactive Ingrowth and Decay of Naturally Occurring Radioactive Materials in the Environment : An Analysis of Produced Fluids from the Marcellus Shale, 123(7), pp. 689–696.
Nyström, J., Dunca, E., Mutvei, H., Lindh, U., 1996. Environmental history as reflected by freshwater pearl mussels in the River Vramsan, southern Sweden. Ambio 25 (5), 350–355.
PADEP, 2023. Oil and Gas Well Waste Report. https://greenport.pa.gov/ReportExtracts/OG/OilGasWellWasteReport.
Parekh, P.P., Khan, A.R., Torres, M.A., Kitto, M.E., 2008. Concentrations of selenium, barium, and radium in Brazil nuts. J. Food Compos. Anal. 21 (4), 332–335. https://doi.org/10.1016/j.jfca.2007.12.001.
Patnode, K.A., Hittle, E., Anderson, R.M., Zimmerman, L., Fulton, J.W., 2015. Effects of high salinity wastewater discharges on unionid mussels in the Allegheny River, Pennsylvania. J. Fish Wildl. Manag. 6 (1), 55–70. https://doi.org/10.3996/052013-JFWM-033 e1944-687X.
Piotrowski, P.K., Tasker, T.L., Geeza, T.J., McDevitt, B., Gillikin, D.P., Warner, N.R., Dorman, F.L., 2020. Forensic tracers of exposure to produced water in freshwater mussels: a preliminary assessment of Ba, Sr, and cyclic hydrocarbons. Sci. Rep. 10 (1) https://doi.org/10.1038/s41598-020-72014-6.

Plexus Scientific Corporation, 2016. Post-Remediation Survey at the Franklin Site Post-Remediation Survey at the Franklin Site Report No. 8284-38E-608.
Pröhl, G., 2003. Framework for Assessment of Environmental Impact Deliverable 3 Dosimetric Models and Data for Assessing Radiation Exposures to Biota.
Ravera, O., Frediani, A., Riccardi, N., 2007. Seasonal variations in population dynamics and biomass of two Unio pictorum mancus (Mollusca, Unionidae) populations from two lakes of different trophic state. J. Limnol. 66 (1), 15–27. https://doi.org/10.4081/jlimnol.2007.15.
Rosenberg, Y.O., Metz, V., Ganor, J., 2011a. Co-precipitation of radium in high ionic strength systems: 1. Thermodynamic properties of the Na-Ra-Cl-SO4-H2O system - estimating Pitzer parameters for RaCl2. Geochim. Cosmochim. Acta 75 (19), 5389–5402. https://doi.org/10.1016/j.gca.2011.06.042.
Rosenberg, Y.O., Metz, V., Oren, Y., Volkman, Y., Ganor, J., 2011b. Co-precipitation of radium in high ionic strength systems: 2. Kinetic and ionic strength effects. Geochim. Cosmochim. Acta 75 (19), 5403–5422. https://doi.org/10.1016/j.gca.2011.07.013.
Rowan, E.L., Engle, M.A., Kirby, C.S., Kraemer, T.F., 2011. Radium content of oil- and gas-field produced waters in the northern Appalachian Basin (USA): summary and discussion of data. http://www.pubs.usgs.gov/sir/2011/5135/.
Ryan, B., Bollhöfer, A., Martin, P., 2008. Radionuclides and metals in freshwater mussels of the upper south Alligator River, Australia. Journal of Environmental Radioactivity 99 (3), 509–526. https://doi.org/10.1016/j.jenvrad.2007.08.019.
Sheppard, S.C., Sheppard, M.I., Ilin, M., Tait, J., Sanipelli, B., 2008. Primordial radionuclides in Canadian background sites: secular equilibrium and isotopic differences. J. Environ. Radioact. 99 (6), 933–946. https://doi.org/10.1016/j.jenvrad.2007.11.018.
Shih, J.S., Saiers, J.E., Anisfeld, S.C., Chu, Z., Muehlenbachs, L.A., Olmstead, S.M., 2015. Characterization and analysis of liquid waste from Marcellus shale gas development. Environ. Sci. Tech. 49 (16), 9557–9565. https://doi.org/10.1021/acs.est.5b01780.
Strayer, D.L., 2014. Understanding how nutrient cycles and freshwater mussels (Unionoida) affect one another. In: Hydrobiologia, Vol. 735, Issue 1. Kluwer Academic Publishers, pp. 277–292. https://doi.org/10.1007/s10750-013-1461-5.
Takesue, R.K., Bacon, C.R., Thompson, J.K., 2008. Influences of organic matter and calcification rate on trace elements in aragonitic estuarine bivalve shells. Geochim. Cosmochim. Acta 72 (22), 5431–5445. https://doi.org/10.1016/j.gca.2008.09.003.
Tasker, T.L., Burgos, W.D., Ajemigbitse, M.A., Lauer, N.E., Gusa, A.V., Kuatbek, M., May, D., Landis, J.D., Alessi, D.S., Johnsen, A.M., Kaste, J.M., Headrick, K.L., Wilke, F.D.H., McNeal, M., Engle, M., Jubb, A.M., Vidic, R.D., Vengosh, A., Warner, N.R., 2019. Accuracy of methods for reporting inorganic element concentrations and radioactivity in oil and gas wastewaters from the Appalachian Basin, U.S. based on an inter-laboratory comparison. Environ. Sci.: Processes Impacts 21 (2), 224–241. https://doi.org/10.1039/c8em00359a.
U.S Environmental Protection Agency, & Engineering and Analysis Division, 2018. Detailed Study of the Centralized Waste Treatment Point Source Category for Facilities Managing Oil and Gas Extraction Wastes (Issue EPA-821-R-18-004).
U.S. Environmental Protection Agency, E. and A. D, 2020. Summary of Input on Oil and Gas Extraction Wastewater Management Practices Under the Clean Water Act.
Van Sice, K., Cravotta, C.A., McDevitt, B., Tasker, T.L., Landis, J.D., Puhr, J., Warner, N. R., 2018. Radium attenuation and mobilization in stream sediments following oil and gas wastewater disposal in western Pennsylvania. Appl. Geochem. 98 (October), 393–403. https://doi.org/10.1016/j.apgeochem.2018.10.011.
Verdegaal, S., 2002. The shell chemistry of Unio crassus batavus as tool for reconstructing the evolution of the Rhine–Meuse delta and its use as indicator for river water composition. Vrije Universiteit, Amsterdam.
Wagner, A., Boman, J., 2004. Biomonitoring of trace elements in Vietnamese freshwater mussels. Spectrochimica Acta - Part B Atomic Spectroscopy 59 (8), 1125–1132. https://doi.org/10.1016/j.sab.2003.11.009.
Warner, N.R., Christie, C.A., Jackson, R.B., Vengosh, A., 2013. Impacts of shale gas wastewater disposal on water quality in Western Pennsylvania. Environ. Sci. Tech. 47 (20), 11849–11857. https://doi.org/10.1021/es402165b.
Wilson, J.M., Vanbriesen, J.M., 2012. Oil and gas produced water management and surface drinking water sources in Pennsylvania. Environ. Pract. 14, 288–300.
Yeager, M.M., Cherry, D.S., Neves, R.J., 1994. Feeding and burrowing behaviors of juvenile rainbow mussels, Villosa iris (Bivalvia:Unionidae). In: Source: Journal of the North American Benthological Society, Vol. 13, Issue 2. https://www.jstor.org/stable/1467240.
Zhao, L., Walliser, E.O., Mertz-Kraus, R., Schöne, B.R., 2017. Unionid shells (Hyriopsis cumingii) record manganese cycling at the sediment-water interface in a shallow eutrophic lake in China (Lake Taihu). Palaeogeography, Palaeoclimatology, Palaeoecology 484, 97–108. https://doi.org/10.1016/j.palaeo.2017.03.010.